

## Bicontinuous Microemulsion-aided Synthesis of Mesoporous TiO<sub>2</sub>

Isamu Moriguchi,<sup>\*,†,††</sup> Yasuko Katsuki,<sup>†</sup> Hirotohi Yamada,<sup>†</sup> Tetsuichi Kudo,<sup>†</sup> and Taisei Nishimi<sup>†††</sup>

<sup>†</sup>Department of Applied Chemistry, Faculty of Engineering, Nagasaki University,  
1-145, Bunkyo-machi, Nagasaki 852-8521

<sup>††</sup>PRESTO JST

<sup>†††</sup>Fuji Photo Film Co. Ltd., 210 Nakanuma, Minami-Ashigara, Kanagawa 250-0193

(Received February 10, 2004; CL-040157)

Mesoporous TiO<sub>2</sub> with high surface area was synthesized via a sol-gel process in a bicontinuous microemulsion. The mesoporous structure was retained to some extent even if the anatase-TiO<sub>2</sub> nanocrystallite produced in the mesophase with heating. The mesoporous anatase-TiO<sub>2</sub> showed an effective Li-intercalation property.

The use of organized systems with surfactant is much attractive to synthesis of nanostructured inorganic materials. For examples, reversed micelles and W/O emulsions have been used for the synthesis of nanoparticles,<sup>1</sup> and in recent years the use of micelle as a template has proven for tailor-making mesoporous materials.<sup>2-5</sup> From the viewpoint of synthesis of porous materials, a bicontinuous microemulsion, which forms in a water/surfactant/oil ternary system with a balanced hydrophilicity and lipophilicity, would be a unique reaction field for the structural regulation. The bicontinuous microemulsions are structured as compartmentalized liquid phases, in which the oil and water phases are separated by surfactant layers into 3-D interconnected nanometer-wide channel networks.<sup>6</sup> The volume and average width of each channel can be controlled with component and composition of water/surfactant/oil. Therefore bicontinuous mesoporous structures of inorganic materials, the pore size and wall thickness of which are tunable in a wide range, are expected to be constructed if a mineralization takes place dominantly in the one compartmentalized phase. However, there are only a few studies related to the bicontinuous microemulsion-aided synthesis to date, and the reported are of syntheses of macroporous frameworks of silica and calcium phosphate.<sup>7-9</sup> In the present work, mesoporous TiO<sub>2</sub> with relatively high surface area was synthesized successfully as the first example of bicontinuous microemulsion-aided synthesis of mesoporous metal oxide. In addition, electrochemical Li-intercalation properties of the mesoporous TiO<sub>2</sub> were also investigated.

A bicontinuous microemulsion was prepared by mixing didodecyldimethylammonium bromide (DDAB), hexane and aq HCl ( $4 \times 10^{-3}$  mol dm<sup>-3</sup>) with the wt % of 34, 36, and 30, respectively.<sup>7,10</sup> The mixture was stirred for 30 min at room temperature until a transparent solution was obtained. Titanium tetrabutoxide (TTB) was added dropwise to the stirred bicontinuous microemulsion with a weight ratio of DDAB:TTB = 3.4:1.4. After further stirring for 30 s and storage at room temperature for 1 day in N<sub>2</sub> atmosphere, the obtained gel was filtered off, washed thoroughly with hexane, dried in an oven at 110 °C for 12 h and finally calcined in air at 300–380 °C for 6 h. In the following, the samples are denoted as BMPT[*x*], where *x* indicates the calcination temperature. The BMPT[300] was slightly brownish, and BMPT[350] and BMPT[380] were colorless,

meaning that almost all the organics were removed by the calcination above 350 °C for 6 h.

On X-ray diffraction (XRD) measurements (Rigaku RINT2200), broad peaks assignable to anatase-TiO<sub>2</sub> were observed on BMPT[350] and BMPT[380] although all the samples showed no distinct XRD peak at  $2\theta/\text{degree} < 10$ . This indicates that the BMPTs did not possess an ordered mesoporous structure like as in micelle-templated mesoporous silica and TiO<sub>2</sub> crystalline phase produced with heating above 350 °C. Nitrogen adsorption-desorption isotherms of the BMPTs, which were measured at 77 K (Micromeritics, Gemini 2370), are compared in Figure 1(i). Pore volume and BJH pore size distribution were calculated using their adsorption branches (Table 1, Figure 1(ii)). The isotherms can be classified into type IV and the inflection characteristic of capillary condensation into mesopores is observed for all the samples at  $0.2 < p/p_0 < 0.5$ , confirming the presence of mesopores. The values of BET surface area of BMPT[300] and BMPT[350] were over 300 m<sup>2</sup> g<sup>-1</sup>, which were higher than the reported on mesoporous TiO<sub>2</sub> synthesized using triblock-copolymer as a template.<sup>3</sup> With increasing *x* (calcination temperature), the BET surface area and mesopore volume of BMPTs decreased and the mean mesopore diameter increased because of the disappearance of small size mesopores below 3 nm in diameter by the sintering. Figure 2 shows transmission electron microscope (TEM, JEOL JEM-2010) images of a precursor gel heated at 110 °C, BMPT[300] and BMPT[380]. Fibrous continuous nanochannels with ca. 5-nm width, which con-

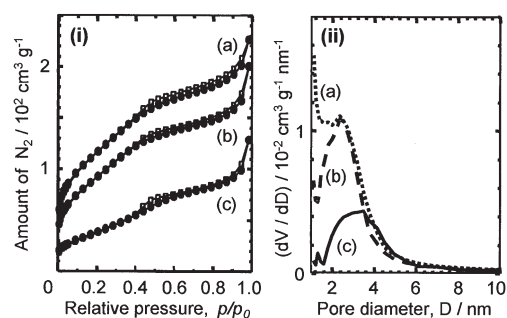


**Figure 1.** (i) Nitrogen adsorption-desorption isotherms and (ii) pore size distributions of BMPTs: (a) BMPT[300], (b) BMPT[350], (c) BMPT[380]. The closed and opened symbols indicate adsorption and desorption processes, respectively.

**Table 1.** Parameters associated with porous structure

Sample	<i>S</i> /m <sup>2</sup> g <sup>-1a</sup>	<i>V</i> /cm <sup>3</sup> g <sup>-1b</sup>	<i>D</i> /nm <sup>c</sup>
BMPT[300]	402	0.40	2.2
BMPT[350]	312	0.34	2.5
BMPT[380]	127	0.21	3.5

<sup>a</sup> BET surface area, <sup>b</sup> Pore volume, <sup>c</sup> Mean mesopore diameter.

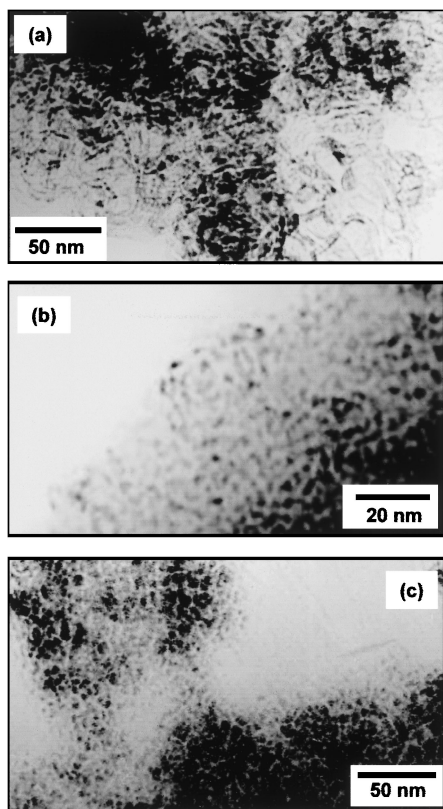


**Figure 2.** TEM images of (a) surfactant/TTB composite gel precursor, (b) BMPT[300] and (c) BMPT[350].

sisted of  $\text{TiO}_2$ -gel wall (black lines in the image) and surfactant (bright parts), were observed for the precursor sample (Figure 2a). This means that  $\text{TiO}_2$ -gel formation occurred preferentially at the water/oil or water/surfactant interface in the bicontinuous microemulsion. On the other hand, a disordered mesoporous structure consisted of continuous nanochannels with 2–4-nm width was confirmed on BMPT[300] (Figure 2b). For BMPT[380], the observed mesoporous structure included nanocrystallites with the size of ca. 6 nm, which was consistent with that determined from the FWHM of XRD peaks of anatase- $\text{TiO}_2$ . These results suggest that fibrous nanochannels in the precursor, which probably reflect the organized structure of bicontinuous microemulsion, changed into the mesoporous structure accompanying the shrinkage of mesopore with heating (removal of organics) and the disappearance of small size mesopores with sintering. It is noteworthy that disordered mesoporous  $\text{TiO}_2$  with relatively high surface area could be obtained by the present method and the mesoporous structure was retained to some extent even if  $\text{TiO}_2$  nanocrystallites produced in the mesoporous phase.

Li-intercalation properties of BMPTs were investigated at room temperature by galvanostatic technique (Hokuto Denko, HZ-3000) using a sealed three-electrode cell equipped with Li counter and reference electrodes. A mixture of BMPT, acetylene black, and polytetrafluoroethylene with a weight ratio of 5:20:2 was pressed onto a nickel mesh and was used as a working electrode. Electrolyte was a 1 mol  $\text{dm}^{-3}$  solution of  $\text{LiClO}_4$  in PC-DME (1:1 by vol.). The cut-off voltages for galvanostatic discharge/charge were set at 3.6 and 1.4 V vs  $\text{Li}/\text{Li}^+$ . Figure 3 shows galvanostatic lithium insertion/extraction curves of

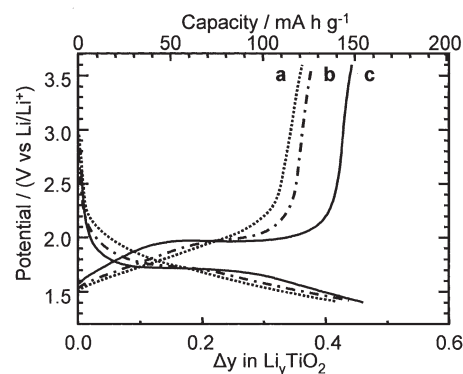


**Figure 3.** Galvanostatic Li-insertion/extraction curves at 1 C of (a) BMPT[300], (b) BMPT[350] and (c) BMPT[380].

BMPTs at the charging rate of 1 C ( $= 0.168 \text{ A g}^{-1}$ ). With increasing  $x$ , the capacity increased and the plateau regions around 1.7 V (insertion process) and 2.0 V (extraction process) appeared and extended. Since the plateaus are related to the phase transition between tetragonal and orthorhombic phases with Li intercalation into anatase- $\text{TiO}_2$ ,<sup>11</sup> the extension of the plateau with increasing  $x$  indicates the increase in crystallinity of mesoporous  $\text{TiO}_2$ . The capacity of BMPT[380] at 1 C was determined from the extraction curve to be  $148 \text{ mA h g}^{-1}$  ( $\text{Li}_{0.44}\text{TiO}_2$ ), which was 88% of the theoretical value of  $168 \text{ mA h g}^{-1}$  assuming the maximum of  $y = 0.5$  in  $\text{Li}_y\text{TiO}_2$ . The estimated capacity was comparable to that of reported on nanocrystalline  $\text{TiO}_2$  electrodes with high surface area.<sup>12,13</sup> These results suggested that the mesoporous  $\text{TiO}_2$  structure resulting from the bicontinuous microemulsion-aided process would be effective to Li-intercalation. Since the process has a potential to control the mesoporous structure in wide range as mentioned in introduction, the present work would contribute to develop functional porous electrode materials such as Li-batteries and supercapacitors.

This work was in part supported by a Grant-in-Aid for Scientific Research from Ministry of Education, Culture, Science, Sports, Technology of Japan. The study made use of instruments (XRD, TEM) in the Center for Instruments Analysis of Nagasaki University.

#### References and Notes

- J. H. Fendler, "Nanoparticles and Nanostructured Films," WILEY-VCH (1998).
- C. T. Kresge, M. E. Leonowicz, W. J. Roth, J. C. Vartuli, and J. S. Beck, *Nature*, **359**, 710 (1992).
- P. Yang, D. Zhao, D. I. Margolese, B. F. Chmelka, and G. D. Stucky, *Chem. Mater.*, **11**, 2813 (1999).
- B. T. Holland, C. F. Blanford, T. Stein, and A. Do, *Chem. Mater.*, **11**, 795 (1999).
- E. L. Crepaldi, G. J. Soler-Illia, D. Grosso, F. Cagnol, F. Ribot, and C. Sanchez, *J. Am. Chem. Soc.*, **125**, 9770 (2003).
- K. Shinoda and B. Lindman, *Langmuir*, **3**, 135 (1978).
- S. D. Sims, D. Walsh, and S. Mann, *Adv. Mater.*, **10**, 151 (1998).
- K. Aikawa, K. Kaneko, T. Tamura, M. Fujitsu, and K. Ohbu, *Colloids Surf., A*, **150**, 95 (1999).
- D. Walsh and S. Mann, *Chem. Mater.*, **8**, 1994 (1996).
- M. Allen, D. F. Evans, D. J. Mitchell, and B. W. Ninham, *J. Phys. Chem.*, **91**, 2320 (1987).
- R. Krol, A. Goossens, and E. A. Meulenkaamp, *J. Electrochem. Soc.*, **146**, 3150 (1999).
- L. Kavan, M. Gratzel, J. Rathousky, and A. Zukal, *J. Electrochem. Soc.*, **143**, 394 (1996).
- For example, Li-insertion ratio  $y$  of nanocrystalline  $\text{TiO}_2$  electrodes was reported to be 0.38 and 0.47 for samples with BET surface area of 145 and  $154 \text{ m}^2 \text{ g}^{-1}$  in powder form, respectively.